Available online at www.sciencedirect.com

SCIENCE DIRECT®

Journal of Molecular Catalysis A: Chemical 206 (2003) 371–387

JOURNAL OF MOLECULAR CATALYSIS A: CHEMICAL

www.elsevier.com/locate/molcata

$Rh_4(CO)_{12}$-derived functionalized MCM-41-tethered rhodium complexes: preparation, characterization and catalysis for cyclohexene hydroformylation

L. Huang*, J.C. Wu, S. Kawi

Chemical and Process Engineering Center, and Department of Chemical and Environmental Engineering, National University of Singapore, 10 Kent Ridge Crescent, Singapore 119260, Singapore

Received in revised form 20 April 2003; accepted 28 May 2003

Abstract

The preparation of $Rh_4(CO)_{12}$-derived functionalized silicate MCM-41-tethered catalysts has been studied by infrared (IR) spectroscopy, X-ray diffraction (XRD) and N_2 adsorption–desorption. Silicate MCM-41 is first functionalized with phosphine, amine and thiol donor ligand groups. Then the functionalized MCM-41 is reacted with $Rh_4(CO)_{12}$ by coordination of surface donor ligands to the rhodium to produce phosphinated and aminated MCM-41-tethered unidentified rhodium carbonyl clusters and MCM-41-tethered $[Rh(\mu\text{-}S(CH_2)_3Si(O_s)_3)(CO)_2]_2$ (where O_s represents surface oxygen). The functionalized MCM-41 and Rh/functionalized MCM-41 possess the structural ordering of mesoporous MCM-41, but exhibit reduced pore sizes, total pore volumes and BET surface areas. The tethered rhodium carbonyl catalysts behave differently with different donor ligands attached in cyclohexene hydroformylation under equimolar CO and H_2 at 2.7 MPa and 100 °C. Only the aminated MCM-41-tethered catalyst displays good activity, selectivity and recycling for the formation of cyclohexane carboxaldehyde. The influences of supported donor ligands on the activity and stability of tethered catalysts for hydroformylation are discussed. The mesoporous structure of MCM-41 is maintained stable during the catalytic reaction.

Keywords: MCM-41; $Rh_4(CO)_{12}$; Functionalization; Tethered catalyst; Cyclohexene hydroformylation

1. Introduction

As a result of the high value of long chain oxygenates as fine chemicals, hydroformylation of cyclohexene has extensively been investigated in both homogeneous and heterogeneous catalysis [1–9]. Thus far, the preparation of heterogeneous hydroformylation catalysts has made use of various supports, such as organic polymers, SiO_2, Al_2O_3, MgO, ZnO, clays, active carbons and zeolites [10–13]. Although zeolites provide an excellent catalyst support with high surface area and unusual catalytic properties, their applications in catalysis are limited by their relatively small pore openings.

The synthesis of the first mesoporous molecular sieves MCM-41 by Mobil's researchers in 1991–1992 opened up the opportunities to apply ordered mesoporous materials to the areas of catalysis, separation, sensors and opto-electric devices. Apart from its high surface area (>700 m^2/g), MCM-41 possesses a hexagonal arrangement of highly uniform sized

* Corresponding author. Present address: Chemical Engineering Department, Laval University, Casier 29, Quebec, Que., Canada G1K 7P4. Tel.: +1-418-6562131; fax: +1-418-6563810.
E-mail address: huanglin1@yahoo.com (L. Huang).

1381-1169/$ – see front matter © 2003 Elsevier B.V. All rights reserved.
doi:10.1016/S1381-1169(03)00423-0

mesopores (15–100 Å) that shows minimal pore size variation. The larger pore sizes of MCM-41 facilitate the flow of reactant and product molecules in and out of the pore system, making them ideal for shape-selective conversions of bulky molecules encountered in the upgrading of heavy residues in refineries and the manufacture of fine chemicals. Within a short period of time, a large number of studies have been made concerning the potential application of MCM-41 in catalysis. The catalytic reactions studied with MCM-41 have involved several industrial reactions of interest, e.g. alkylation, cracking, selective oxidations including epoxidation, alkene oligomerization, NO_x selective reduction and benzene hydrogenation [14,15]. MCM-41-based catalysts have been found to have higher performances in these processes than conventional zeolite- and oxide-based catalysts.

The high activities are generally attributed to the high surface area and narrow mesopore size distribution of MCM-41. However, to our knowledge, very few papers have appeared on the catalytic application of MCM-41 in hydroformylation up to date [16]. The mesoporous framework of MCM-41 not only can be freely accessible to large reactant molecules but favors immobilizing large amounts of metallic components or molecular metallic complexes.

Immobilization of metallic and organometallic complex catalysts is viewed as an important and practical issue for the separation and recycling of catalysts in the industrial reaction processes. As far as the preparation of inorganic support-immobilized rhodium hydroformylation catalysts is concerned, organometallic complexes and inorganic salts are usually utilized to adsorb directly on oxides, such as SiO_2, Al_2O_3, MgO and ZnO, and zeolites so as to obtain supported rhodium complex catalysts and supported rhodium metallic catalysts. However, the supported catalysts thus produced often face the problem of leaching of rhodium catalytic components during hydroformylation reactions, depending on the strength of the interaction between catalyst precursors and surface OH groups. Particularly on the weakly acidic surfaces of SiO_2 and other silicates, all rhodium catalyst precursors remain physisorbed without chemical linkage to the surfaces. This doubtless cannot prevent rhodium complexes, which are soluble in organic solvents, from being extracted from the surfaces when operated under the liquid phase hydroformylation conditions. To achieve organometallic complexes or inorganic compounds chemically linked to the surfaces of SiO_2 and other silicates, one must make use of ligand silane coupling reagents which function as linkers to tether organometallic complexes or inorganic compounds to the surfaces [17]. A great number of studies have been published on the preparation of organometallic complexes or inorganic compounds tethered to SiO_2 and mesoporous molecular sieves by using organosilane coupling reagents [9,16,18–49]. The organosilanes play roles in promoting the catalysis of organometallic or inorganic compounds as well as in grafting these compounds on the surfaces. The commonly used organosilanes contain phosphorus, nitrogen and sulfur. Some of these tethered rhodium complexes have been recognized as hydroformylation catalyst precursors [4,9,16,19,20,29,31,36,37,41,44].

Until now, only a limited number of studies have been reported concerning hydroformylation catalysts prepared by linkage of phosphine-free rhodium complexes, such as $Rh(acac)(CO)_2$ and $[RhCl(CO)_2]_2$ to SiO_2 using phosphines, amines and thiols [19,20]. The effects of the three donor ligands on the catalytic properties in hexene-1 hydroformylation were briefly evaluated and compared. Nevertheless, there has been no detailed description on the stability and recycling of the heterogenized catalysts including rhodium loss by leaching under reaction conditions.

In this work, we aimed to explore the preparative processes of rhodium carbonyls tethered to MCM-41 from $Rh_4(CO)_{12}$ by use of phosphorus-, nitrogen- and sulfur-containing organosilane coupling reagents. We attempted to achieve active, selective and stable MCM-41-tethered rhodium complex catalysts toward cyclohexene hydroformylation for the first time. We also intended to understand the promotional effects of different donor ligands coordinated to the rhodium on the catalytic hydroformylation as well as the stabilization of them on the tethered rhodium complex catalysts.

2. Experimental

Sodium silicate solution (25.5–28.5% SiO_2, 7.5–8.5% Na_2O) and *N*-cetyl-*N*,*N*,*N*-trimethylammonium bromide (CTMABr, 98–101%) and cyclohexene (99%) were purchased from Merck. Tetraethylam-

monium hydroxide solution (TEAOH, 20%) was obtained from Sigma. (3-Chloropropyl)trimethoxysilane ($Cl(CH_2)_3Si(OMe)_3$, 97%), (3-aminopropyl)triethoxysilane ($H_2N(CH_2)_3Si(OEt)_3$, 99%), (3-mercaptopropyl)trimethoxysilane ($HS(CH_2)_3Si(OMe)_3$, 96%) and potassium diphenylphosphide ($KPPh_2$, 0.5 M solution in tetrahydrofuran (THF)) were supplied by Aldrich. Tetrarhodium dodecacarbonyl ($Rh_4(CO)_{12}$, 98%) was supplied by Strem. All other reagents were purchased commercially. Organic solvents were distilled and dried prior to use. The gases $CO + H_2$ and N_2 had a purity of 99.999%.

Silicate MCM-41 was synthesized as described below. 79.6 g of sodium silicate solution and 50 g of distilled water were added to a solution containing 64.4 g of CTMABr and 130 ml of TEAOH. After stirring for 10 min to form a gel, 1 M H_2SO_4 was added to the gel and the pH value adjusted to 9.5–10. Additional water was added to make the following molar ratio of the final gel composition—SiO_2:CTMABr:TEAOH:Na_2O:H_2O (1.0:0.48:0.48:0.39:50). The gel mixture was stirred for 2 h at room temperature, transferred into a polypropylene bottle and then statically heated at 96 °C for 4 days under autogenerated pressure. The final solid material obtained was filtered off, washed with distilled water until free of bromide ions, dried and calcined in an oven at 560 °C for 10 h. In order to regenerate sufficient amounts of OH groups on the MCM-41 surface, the calcined MCM-41 was exposed to air at room temperature for 2 days followed by dehydration at 200 °C for 5 h.

To functionalize silicate MCM-41, 10 ml of organosilane was mixed with 2.0 g of MCM-41 in 150 ml of toluene. The mixture was refluxed under N_2 for 16 h. The resulting solid was filtered off, washed with 200 ml of chloroform and dried in vacuum. The chlorinated, aminated and thiolated MCM-41 samples thus prepared contained 5.5% Cl, 3.7% N and 5.0% S, respectively. The chlorinated MCM-41 was further refluxed with 1 ml of $KPPh_2$ in 25 ml of THF under N_2 for 1 h. After filtration, washing with 100 ml of methanol and drying in vacuum, the resulting phosphinated MCM-41 contained 0.2% Cl and 4.0% P. Chlorinated, phosphinated, aminated and thiolated MCM-41 samples are denoted as MCM-41(Cl), MCM-41(PPh_2), MCM-41(NH_2) and MCM-41(SH), respectively.

Supported catalyst precursors were prepared as follows. One gram of unfunctionalized or functionalized support was impregnated with a solution of $Rh_4(CO)_{12}$ (37 mg) in *n*-hexane under N_2. The system was stirred at room temperature under N_2 for 5 h. In the case with unfunctionalized MCM-41, the solid powder turned light red in color and the red color of the solution remained unchanged at the end of stirring. In the case with functionalized MCM-41, the solid powder colorated and the red solution became colorless rapidly after stirring. MCM-41(PPh_2), MCM-41(NH_2) and MCM-41(SH) turned deep brown, brown and yellow in color, respectively, after reactions with $Rh_4(CO)_{12}$. Afterward, the liquid was drawn off with a syringe under N_2 and the resulting solid was washed three times with *n*-hexane under N_2 followed by drying under vacuum (1.3×10^{-6} MPa).

Hydroformylation of cyclohexene was conducted under 2.7 MPa of an equimolar CO and H_2 mixture at 100 °C in an autoclave. Three hundred milligrams of catalyst precursor, 12 ml of cyclohexene and 55 ml of THF were first transferred to the autoclave inside a glove box. Subsequently, the $CO + H_2$ mixture was charged after the reaction system had been purged with this reaction gas mixture. Sampling of the reaction mixture was done during the course of reaction.

Infrared (IR) spectroscopy experiments were carried out on a Shimadzu 8700 FTIR spectrometer at a resolution of 4 cm^{-1}. The solid samples studied were pressed into wafers of 15 mg each and placed in a single beam IR cell where the wafers could be subjected to the desired treatments. In situ IR spectroscopic studies of the reactivities between $Rh_4(CO)_{12}$ and unfunctionalized or functionalized MCM-41 were performed by dripping $Rh_4(CO)_{12}$ solution on unfunctionalized or functionalized MCM-41 wafers under N_2. IR spectra of supported rhodium complexes were recorded by subtracting the support contribution.

X-ray diffraction (XRD) of unfunctionalized and functionalized MCM-41 was performed on a Shimadzu XRD-6000 spectrometer with Cu Kα monochromatic radiation. N_2 adsorption–desorption experiments were done on a Quantachrome Autosorb-1 (AS-1) analyzer. The rhodium contents of the samples were determined by atomic absorption spectroscopy. The chlorine, sulfur and phosphorus contents of the samples were analyzed by X-ray fluorescence. Thermogravimetric analysis (TGA) was used to

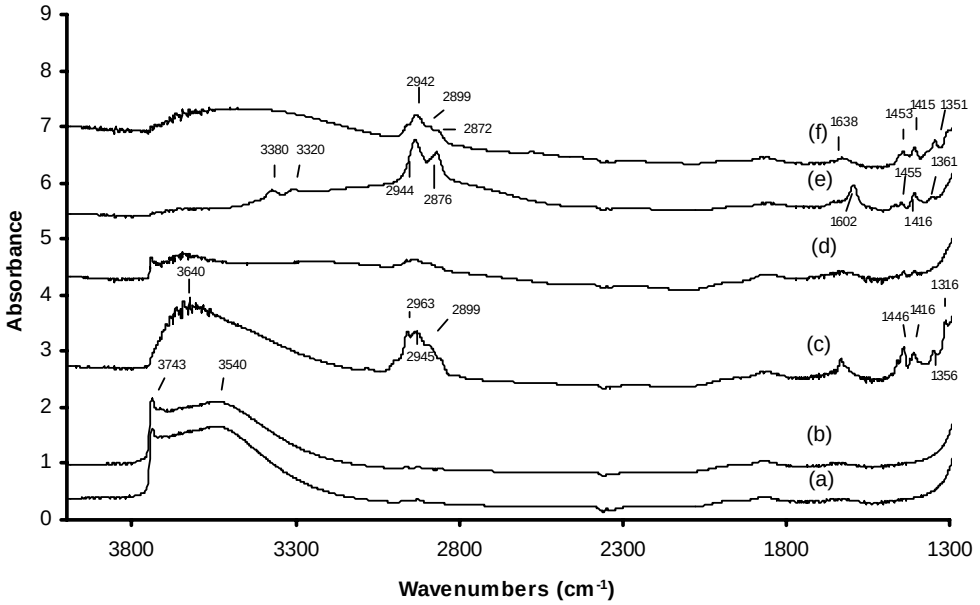

Fig. 1. IR spectra of: (a) MCM-41; (b) Rh/MCM-41; (c) MCM-41(Cl); (d) MCM-41(PPh_2); (e) MCM-41(NH_2); (f) MCM-41(SH).

estimate the contents of chlorine, nitrogen and sulfur in MCM-41(Cl), MCM-41(NH_2) and MCM-41(SH).

3. Results and discussion

3.1. Studies of the preparative processes of MCM-41-tethered rhodium carbonyls

3.1.1. By IR spectroscopy

Fig. 1 shows the IR spectra of the vibrations of MCM-41-based sample wafers after dehydration at 200 °C under vacuum (1.3×10^{-9} MPa) for 2 h. In order for the observation of the vibrations of surface OH groups, dehydration at 200 °C is required to enable physisorbed molecular water to largely eliminate from the MCM-41 surface and thus make bands for surface OH groups appear in the spectrum. The surface of MCM-41 contains a large amount of OH groups, which are characterized by a narrow band at 3743 cm^{-1} and a very broad band centered at 3532 cm^{-1}. The surface spectrum of Rh/MCM-41 (2% Rh loading) derived from $Rh_4(CO)_{12}$ is quite similar to that of MCM-41. This implies that no chemical bond Rh–OSi is formed at the expense of surface OH groups when $Rh_4(CO)_{12}$ is deposited on the MCM-41 surface. After MCM-41 had been functionalized with $Cl(CH_2)_3Si(OMe)_3$, the band at 3743 cm^{-1} for OH groups depleted greatly in favor of the appearance of bands at 2963, 2945, 2899, 1446, 1416, 1356 and 1316 cm^{-1}. These bands are ascribed to the vibrations of alkyl group in the silane. The remaining broad band centered at 3624 cm^{-1} corresponds to molecular water which is believed to strongly adsorb on the Cl-containing MCM-41 surface and not to evacuate at 200 °C. After Cl had been substituted with PPh_2, this broad band no longer appeared, proving the strong adsorption of molecular water on the Cl-containing MCM-41 surface. In the case of MCM-41(NH_2), the bands for OH groups nearly disappeared. At the same time, a series of new bands at 3380, 3320, 2944, 2876, 1602, 1455 and 1416 cm^{-1} appeared. The bands at 3384, 3320 and 1602 cm^{-1} are assigned to the vibrations of NH_2 group. The bands at 2944, 2876, 1455, 1416 and 1361 cm^{-1} are attributed to the vibrations of alkyl group in the silane. In the case of MCM-41(SH), a similar change was observed in the spectrum. The 1638 cm^{-1} band is attributed to the vibration of SH group. The bands at 2942, 2899, 2872, 1453, 1415 and 1351 cm^{-1} are likewise due to the vibrations of alkyl group.

The above IR spectroscopic results suggest that the significant condensation occurs between the OH groups present at the surface of MCM-41 and the organosilanes to form surface silanol species as below:

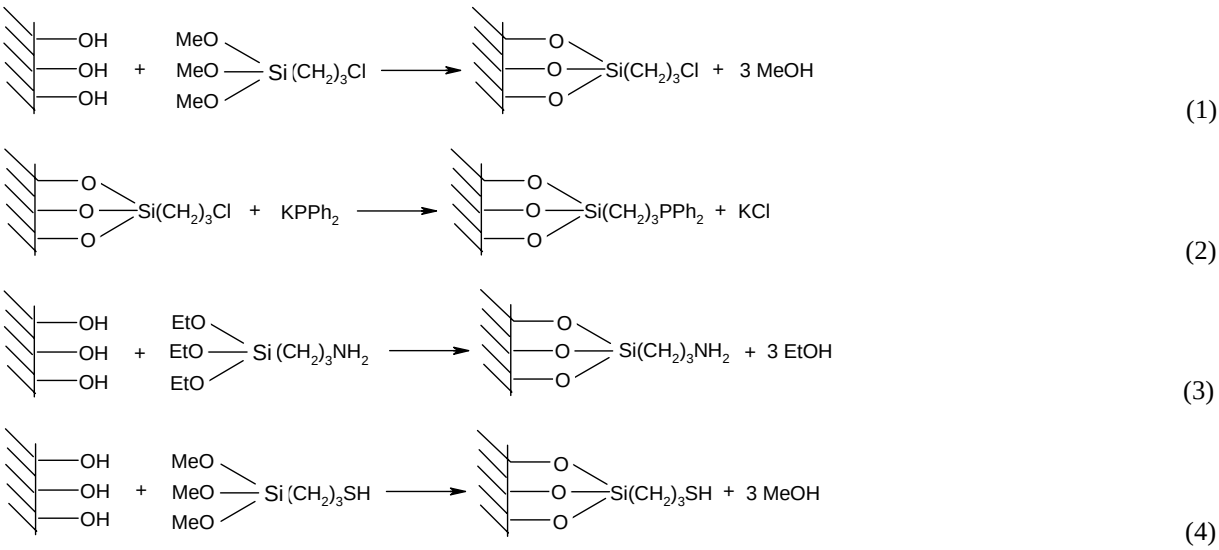

The greater band depletion of OH groups observed in the case of MCM-41(NH_2) is interpreted in terms of the stronger reactivity of ethyl group with surface OH group. This is also reflected in the higher grafted silane content in MCM-41(NH_2) estimated by TGA.

In Fig. 2 and Table 1 are presented the IR spectroscopic data after the interactions of $Rh_4(CO)_{12}$ with the surfaces of unfunctionalized and functionalized MCM-41. As soon as a wafer of MCM-41 predehydrated at 200 °C which was placed in the IR cell was impregnated with a red solution of $Rh_4(CO)_{12}$

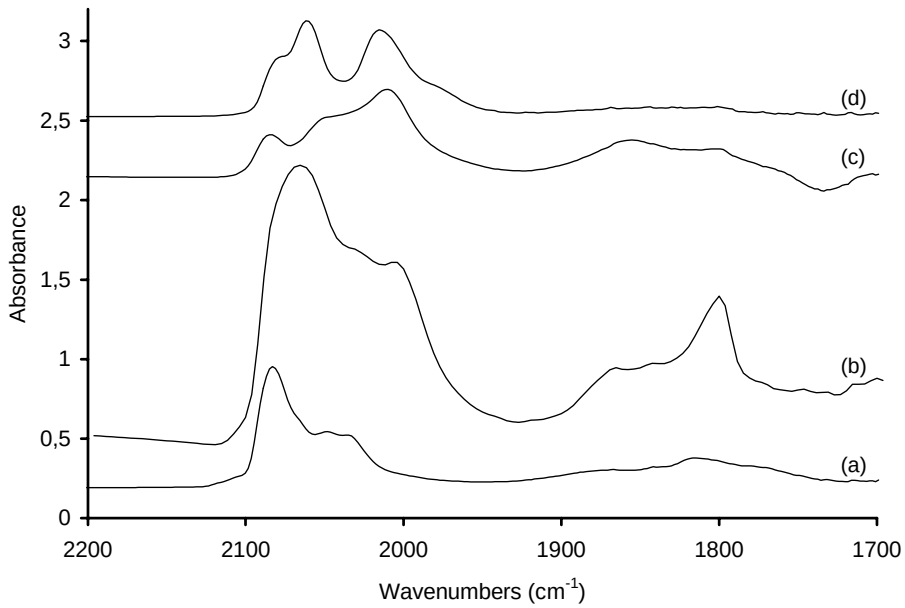

Fig. 2. IR spectra after impregnation of support with $Rh_4(CO)_{12}$/*n*-hexane under N_2 followed by 1 h of treatment under vacuum (1.3×10^{-9} MPa) of: (a) $Rh_4(CO)_{12}$/MCM-41; (b) $Rh_4(CO)_{12}$/MCM-41(PPh_2); (c) $Rh_4(CO)_{12}$/MCM-41(NH_2); (d) $Rh_4(CO)_{12}$/MCM-41(SH).

Table 1
IR spectroscopic data of rhodium carbonyl complexes

Complex	υ(CO) (cm^{-1})	Reference
$Rh_4(CO)_{12}$/*n*-hexane	2069s, 2044m, 1886m	This work
$Rh_6(CO)_{16}$/Nujol mull	2105w, 2070s, 2047w, 2040w, 2022mw, 2020mw, 1833w, 1793s	[50]
$Rh_6(CO)_{16}$/KBr	2073s, 2026m, 1800s	[51]
$Rh_6(CO)_{16}/SiO_2$	2083s, 2051m(sh), 1804m(br)	[52]
$Rh_4(CO)_{12}$/MCM-41	2084s, 2069sh, 2052m, 2034m, 1885w(br), 1816m(br)	This work[a]
$Rh_4(CO)_{12}$/MCM-41(PPh_2)	2065s(br), 2030m(br), 2003m(br), 1869w(br), 1800m(br)	This work[a]
$Rh_4(CO)_{12}$/MCM-41(NH_2)	2086m, 2052m(sh), 2013s, 1857m(br), 1801w(br)	This work[a]
$Rh_4(CO)_{12}$/MCM-41(SH)	2079m(sh), 2063s, 2017s, 1978w(sh)	This work[a]
$[Rh(\mu\text{-}S(CH_2)_3Si(OMe)_3)(CO)_2]_2/SiO_2$	2081m, 2064s, 2020s	[41]
$[Rh(\mu\text{-}S(CH_2)_3Si(OMe)_3)(CO)_2]_2$/*n*-hexane	2071m, 2052s, 2003s, 1972vw	This work[b]
$[Rh(\mu\text{-}S(CH_2)_3Si(OMe)_3)(CO)_2]_2$/toluene	2074m, 2056s, 2004s	[41]

[a] By impregnation of support with $Rh_4(CO)_{12}$/*n*-hexane under N_2 followed by 1 h of treatment under vacuum (1.3×10^{-6} MPa).
[b] By 2 h of reaction between $Rh_4(CO)_{12}$ and four equivalents of $HS(CH_2)_3Si(OMe)_3$ in *n*-hexane.

in *n*-hexane under N_2, the wafer color turned red and the surface spectrum exhibited carbonyl bands at 2081s, 2069sh, 2046m, 2030m, 1885m(br) and 1822w(br) cm^{-1}. The bands at 2069, 2046 and 1885 cm^{-1} represent the carbonyl vibrations of $Rh_4(CO)_{12}$. The appearance of the bands at 2081, 2030 and 1822 cm^{-1} is attributed to the formation of $Rh_6(CO)_{16}$ on the surface. After removal of the solvent, the bands characteristic of supported $Rh_4(CO)_{12}$ depleted in favor of those of supported $Rh_6(CO)_{16}$ as the interaction time increased. Finally, the wafer color remained red and the surface spectrum consisted of the bands of supported $Rh_6(CO)_{16}$ as the major supported component and the bands of supported $Rh_4(CO)_{12}$ as the minor supported component, as shown in Fig. 2(a). In a separate impregnation experiment involving the powder sample depicted in Section 2, the solution color still remained red although the solid color turned red after a prolonged stirring of a *n*-hexane solution of $Rh_4(CO)_{12}$ with the MCM-41 powder.

The above observations reveal that $Rh_4(CO)_{12}$ converts spontaneously to $Rh_6(CO)_{16}$ upon contact with the unfunctionalized MCM-41 surface [52], consistent with the formation of no Rh–OSi bond mentioned before. This result almost coincides with what has occurred on the SiO_2 surface [53]. The reaction:

$$3Rh_4(CO)_{12} \rightarrow 2Rh_6(CO)_{16} + 4CO \quad (5)$$

is well known to be quickly completed on the surface of SiO_2 under vacuum [53,54]. The slight difference observed on MCM-41 is that the product mixture still contains a fraction of unreacted $Rh_4(CO)_{12}$, possibly due to the influence of mesopore channels on the transformation of $Rh_4(CO)_{12}$.

Upon addition of a *n*-hexane solution of $Rh_4(CO)_{12}$ under N_2 onto a wafer of MCM-41(PPh_2) predehydrated at 200 °C, the wafer color turned deep brown at once and the surface spectrum exhibited three linear carbonyl bands at 2080m, 2053m and 2003m cm^{-1} and an ill-resolved broad bridged carbonyl band. After removal of the solvent, the spectrum became intense and bridged carbonyl bands emerged at 1869w and 1800m cm^{-1} as seen in Fig. 2(b). This spectrum does not correspond to either that of supported $Rh_4(CO)_{12}$ or that of supported $Rh_6(CO)_{16}$. We attribute it to a new grafted rhodium carbonyl cluster not identified, since bridged carbonyl bands are still retained. In a separate impregnation experiment stated in experimental part, the solid phase turned deep brown in color and the liquid phase became colorless immediately after the MCM-41(PPh_2) powder had been stirred with a *n*-hexane solution of $Rh_4(CO)_{12}$.

When a *n*-hexane solution of $Rh_4(CO)_{12}$ was brought in contact under N_2 with a wafer of MCM-41(NH_2) predehydrated at 200 °C, the wafer color turned brown immediately. The surface spectrum showed three linear carbonyl bands at 2086m, 2052s and 2013s cm^{-1} and two bridged carbonyl bands near 1857m(br) and 1801m(br) cm^{-1}. After removal of the solvent, the 2086 cm^{-1} band remained unchanged whereas the 2052 cm^{-1} band depleted with the concomitant growth of the 2013 and 1859 cm^{-1} bands as the interaction between the cluster and the support proceeded, as seen in Fig. 2(c). The spectral pattern

resembled neither that of supported $Rh_4(CO)_{12}$ nor that of supported $Rh_6(CO)_{16}$. It may be related to a new supported rhodium carbonyl cluster, since bridged carbonyl ligands were still observed. In a separate impregnation experiment involving the powder sample depicted in Section 2, the powder color turned brown and the solution became colorless rapidly after stirring of the MCM-41(NH_2) powder with a *n*-hexane solution of $Rh_4(CO)_{12}$.

Similarly, a *n*-hexane solution of $Rh_4(CO)_{12}$ was dripped under N_2 onto a wafer of MCM-41(SH) predehydrated at 200 °C. The wafer color turned yellow immediately. Meanwhile, the surface spectrum displayed four linear carbonyl bands at 2079m, 2059s, 2013s and 1972sh cm^{-1}. Both position and relative intensity of these three bands are quite similar to those for $[Rh(\mu\text{-}S(CH_2)_3Si(O_s)_3)(CO)_2]_2$ on SiO_2 (2081m, 2064s and 2020s cm^{-1}), which was reported by Gao and Angelici to be formed from $[Rh(CO)_2Cl]_2$ and $HS(CH_2)_3Si(OMe)_3$ [41]. In a parallel impregnation experiment involving the powder sample described in Section 2, the solution turned colorless quickly in favor of the solid color change into yellow after stirring of the MCM-41(SH) powder with $Rh_4(CO)_{12}$ solution. Thus, we suggest that an identical rhodium carbonyl dimer is formed on the surface of MCM-41. In order to conform this hypothesis, we run a homogeneous reaction of $Rh_4(CO)_{12}$ with $HS(CH_2)_3Si(OMe)_3$ in *n*-hexane. $Rh_4(CO)_{12}$ and four equivalents of $HS(CH_2)_3Si(OMe)_3$ produced a deep red mixture under N_2 which gave an IR spectrum containing four linear carbonyl bands at 2071m, 2052s, 2003s and 1972vw cm^{-1} as shown in Fig. 3. We assign this spectrum to $[Rh(\mu\text{-}S(CH_2)_3Si(OMe)_3)(CO)_2]_2$ as this spectrum matches with that of $[Rh(\mu\text{-}S(CH_2)_3Si(OMe)_3)(CO)_2]_2$ in toluene (2074m, 2056s and 2004s cm^{-1}) and the spectral pattern of $[Rh(\mu\text{-}SR)_2(CO)_2]_2$ (R = Me, C_6H_5, *p*-FC_6H_4) in solvents reported before [41,55]. This solution spectrum is entirely compatible with the surface spectrum.

As far as we know, the organometallic chemistry of $Rh_4(CO)_{12}$ with nitrogen and sulfur donor ligands is unpublished. From the above IR spectroscopic monitoring of the reactivities of $Rh_4(CO)_{12}$ with supported phosphine, amine and thiol ligands, we

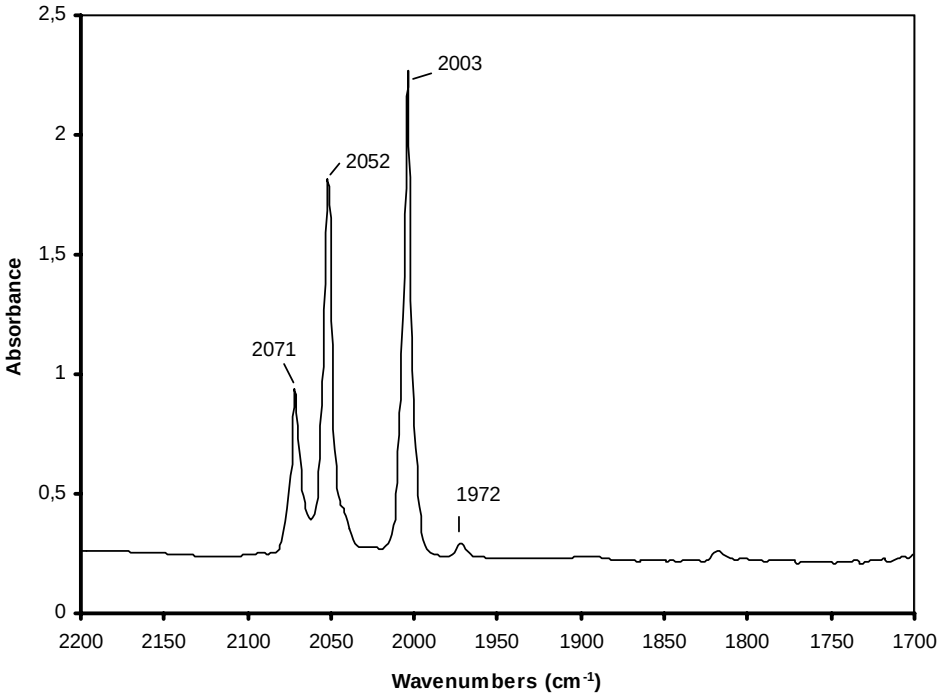

Fig. 3. IR spectrum of the reaction mixture between $Rh_4(CO)_{12}$ and four equivalents of $HS(CH_2)_3Si(OMe)_3$ in *n*-hexane after 2 h.

realize that supported thiol ligand reacts the most strongly with $Rh_4(CO)_{12}$ to render the cluster disintegrated and the rhodium atoms oxidized, while supported phosphine and amine ligands do not appear to make the cluster break down when coordinated to the rhodium atoms. It is noticed through a careful comparison of Fig. 2(b) and (c) that the bridged band around 1800 cm^{-1} is much more prominent with $Rh_4(CO)_{12}$/MCM-41(PPh_2) than with $Rh_4(CO)_{12}$/MCM-41(NH_2). This indicates that the rhodium cluster transfers more increased negative charge from the phosphorus to CO due to the presence of a poorer π-electron acceptor than CO and less increased negative charge from the nitrogen to CO because of the strong electronegativity of the nitrogen. The stronger dπ–pπ bonding between the rhodium and CO in $Rh_4(CO)_{12}$/MCM-41(PPh_2) than in $Rh_4(CO)_{12}$/MCM-41(NH_2) suggests that CO ligands are bonded more strongly to the rhodium atoms in the presence of a phosphine ligand coordinated than in the presence of an amine ligand coordinated. The IR spectroscopic characterization results will help us get a better understanding of catalytic performances and stability of MCM-41-tethered rhodium complexes via different donor ligands in cyclohexene hydroformylation.

3.1.2. By X-ray diffraction

The XRD spectrum of unfunctionalized MCM-41 exhibits an intense diffraction peak at a low angle ($2\theta = 2.16^\circ$) representing the d_{100} reflection line and two additional weak diffraction peaks at higher angles ($2\theta = 3.80$ and 4.36°) representing d_{200} and d_{210} reflection lines, consistent with the characteristics of standard MCM-41 [56]. Rh/MCM-41 had a XRD spectrum characteristic of MCM-41 with peak intensities comparable to those for unfunctionalized MCM-41. This is true for demonstrating that the direct deposition of Rh on the channel walls of MCM-41 from $Rh_4(CO)_{12}$ leads to no change in the mesoporous structure of MCM-41 without the involvement of any chemical reaction between $Rh_4(CO)_{12}$ and silanol groups of MCM-41, in nice agreement with the IR spectroscopic results. Meanwhile, it should be considered that a deposited amount of Rh as low as 2% on MCM-41 may affect the mesoporous structure negligibly. After silylation of MCM-41, the XRD spectra of the resulting MCM-41(Cl), MCM-41(NH_2) and MCM-41(SH) obviously displayed decreased peak intensity. Accordingly, it may be assumed that silylation of MCM-41 channels somewhat reduces mesopore size uniformity, but substantially does not alter mesoporous structural ordering. When Cl was replaced with PPh_2 in MCM-41(Cl), the XRD peak intensities of the resulting MCM-41(PPh_2) continued to diminish. This may be due to the presence of larger PPh_2 ligands in the MCM-41 channels which further reduces mesopore size uniformity. Grafting of Rh on the three functionalized MCM-41 samples from $Rh_4(CO)_{12}$ resulted in weak decrease in XRD spectral intensity, probably because of the small amount of Rh coordinating the functional groups.

3.1.3. By N_2 adsorption–desorption

Figs. 4–6 show the N_2 adsorption–desorption isotherms of MCM-41-based powdered samples. Based on the N_2 adsorption branch data, the pore sizes, total pore volumes and BET surface areas are obtained (Table 2). Our unfunctionalized MCM-41 sample displayed a typical type IV mesoporous adsorption–desorption behavior, agreeing with a known standard N_2 adsorption–desorption isotherm of MCM-41 [56]. The uniform MCM-41 mesopores led to a narrow pore size distribution having a pore diameter (D_{BJH}) around 30 Å. Rh/MCM-41 gave a similar type IV mesoporous adsorption–desorption isotherm and a narrow pore size distribution, although its capillary condensation step emerged at slightly lower relative pressure. Deposition of Rh on MCM-41 only caused a weak reduction of mean pore diameter from 30 to 28 Å and slight decreases of pore volume and

Table 2
Physical properties of unfunctionalized and functionalized MCM-41

Sample	Pore diameter (Å)	Total pore volume (cm^3/g)	BET surface area (m^2/g)
MCM-41	30	1.29	1651
Rh/MCM-41	28	1.14	1579
MCM-41(Cl)	19	0.48	712
MCM-41(PPh_2)	18	0.31	460
Rh/MCM-41(PPh_2)	<18	0.36	426
MCM-41(NH_2)	19	0.43	726
Rh/MCM-41(NH_2)	20	0.41	756
MCM-41(SH)	24	0.78	1487
Rh/MCM-41(SH)	24	0.76	1430

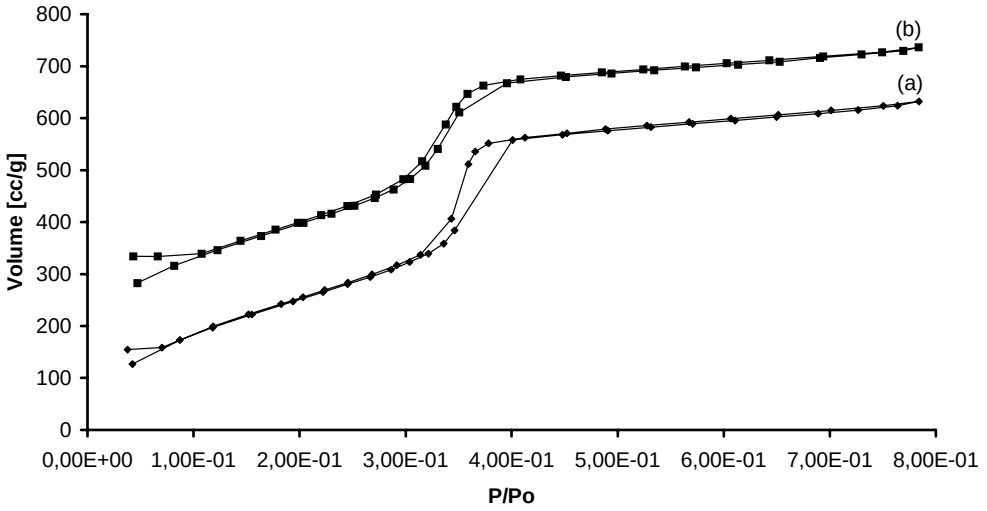

Fig. 4. N_2 adsorption–desorption isotherms of: (a) MCM-41; (b) Rh/MCM-41.

surface area, probably because of the weak amount of Rh dispersed on the mesoporous channel walls. These are consistent with the IR spectroscopic and XRD results. In contrast, MCM-41(Cl), MCM-41(NH_2) and MCM-41(SH) prepared by silylation showed adsorption–desorption isotherms with the capillary condensation steps obviously shifting to lower relative pressures and pore size distributions evidently shifting to lower pore diameters. Functionalization of MCM-41 resulted in not only important reduction of mean pore diameter but remarkable decreases of pore volume and surface area. Therefore, the observed adsorption–desorption isotherms that deviated from that of MCM-41 may be interpreted in terms of strong pore filling with the organosilanes having larger chemical ligands. Replacement of Cl with PPh_2 produced further decreases in these parameters. The observed changes correlate with the organosilane's size. The greater change took place with $Ph_2P(CH_2)_3Si(OMe)_3$ which has a larger size. However, introduction of

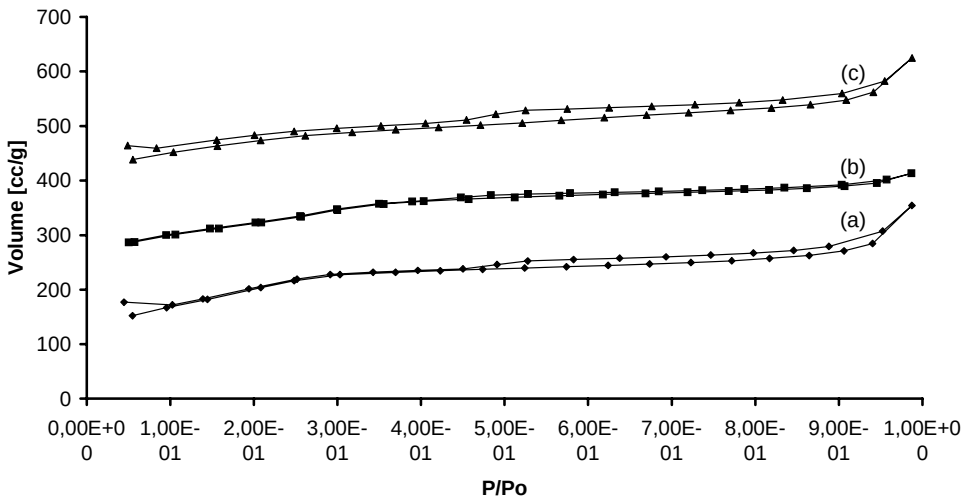

Fig. 5. N_2 adsorption–desorption isotherms of: (a) MCM-41(Cl); (b) MCM-41(PPh_2); (c) Rh/MCM-41(PPh_2).

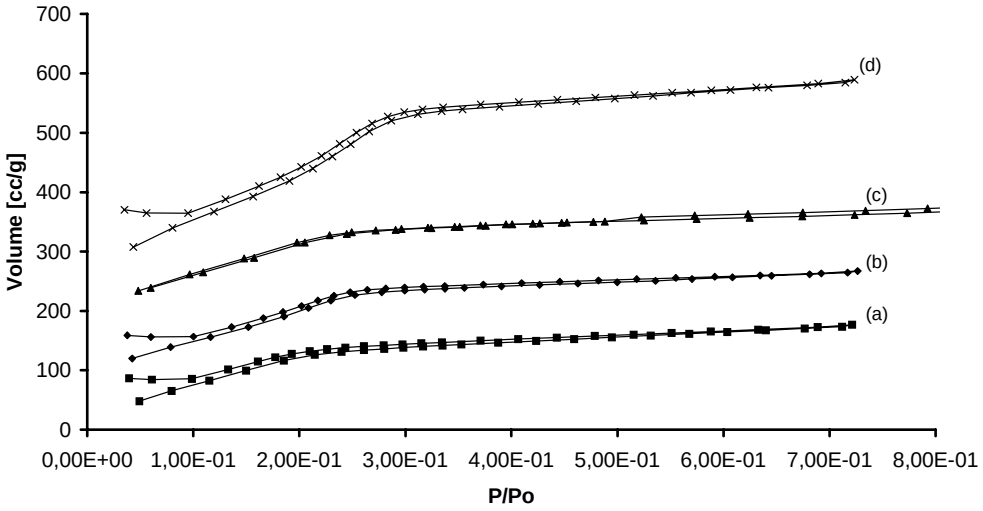

Fig. 6. N_2 adsorption–desorption isotherms of: (a) MCM-41(NH_2); (b) Rh/MCM-41(NH_2); (c) MCM-41(SH); (d) Rh/MCM-41(SH).

Rh to the mesopore channels by complexation with phosphine, amine and thiol ligands led to little modification of the properties of N_2 adsorption–desorption, due to the limited amount of Rh used.

3.2. Studies of catalytic cyclohexene hydroformylation

All the catalyst precursors were tested in cyclohexene hydroformylation which was run at 2.7 MPa and 100 °C in an autoclave. Table 3 presents the comparative catalytic results at the end of 20 h of reaction over these catalyst systems. The blank test showed no catalytic activities in this autoclave. All the catalysts studied displayed selectivities greater than 98% to cyclohexane carboxaldehyde with formation of no alcohols under reaction conditions.

When $Rh_4(CO)_{12}$/MCM-41(NH_2) was used as a catalyst precursor, a turnover of 1610 mol/mol Rh for cyclohexene converted was obtained in the first

Table 3
Catalytic properties of $Rh_4(CO)_{12}$-derived catalysts[a] in cyclohexene hydroformylation[b]

Catalyst precursor	Conversion (%)	Turnover[c] (mol/mol Rh)	Product distribution (mol%)	
			Cyclohexane	Cyclohexane carboxaldehyde
$Rh_4(CO)_{12}$[d]	86.5	1743	0	100
$Rh_4(CO)_{12}$/MCM-41	92.8	2009	1.7	98.3
$Rh_4(CO)_{12}$/MCM-41(NH_2)				
First cycle	73.2	1610	1.5	98.5
Second cycle	65.5	1596	0.5	99.5
Third cycle	77.2	1904	0.6	99.4
$Rh_4(CO)_{12}$/MCM-41(PPh_2)				
First cycle	20.1	440	1.3	98.7
Second cycle	0.8	465	1.0	99.0
$Rh_4(CO)_{12}$/MCM-41(SH)	0	–	–	–

[a] 0.30 g of catalyst precursor with nearly 2.0% Rh loading.
[b] Reaction conditions: 2.7 MPa, 100 °C, $H_2/CO = 1$, 20 h per cycle.
[c] For conversion of cyclohexene.
[d] 0.011 g.

reaction cycle, 98.5% of which was hydroformylated to cyclohexane carboxaldehyde and only 1.5% of which was hydrogenated to cyclohexane. Accordingly, the $Rh_4(CO)_{12}$-derived MCM-41(NH_2)-tethered catalyst is fairly active for cyclohexene hydroformylation. When a reaction cycle of 20 h ended, the solid sample was filtered off from the reaction mixture in air. After the first cycle, the solid sample color remained brown and the liquid phase color turned light brown. According to the results of elemental analysis (Table 4), 1.67% of Rh was retained on the solid sample. This accounts for a weak loss of surface amine ligand bonded rhodium catalytic components from the support relative to the initial rhodium loading of 1.85% during the first cycle. In the second cycle, the catalytic hydroformylation activity was noted to slightly decrease due to the slight loss of catalytic components from the support during the first cycle. The solid sample color still remained brown and the liquid phase was colorless after reaction. Simultaneously the rhodium content of solid sample no longer diminished. In the third cycle, the catalytic hydroformylation activity was found to significantly increase which was higher than that of a homogeneous catalyst derived from $Rh_4(CO)_{12}$, with no change in rhodium content of solid sample. The results demonstrate that the MCM-41(NH_2)-tethered rhodium carbonyl catalyst is stable for recycling without obvious rhodium leaching as well as active in cyclohexene hydroformylation, owing to the proper coordinative bonding between the surface amine and the rhodium center.

Table 4
Color and rhodium content changes of supported rhodium carbonyls samples before and after cyclohexene hydroformylation

Catalyst precursor	Before reaction		After reaction	
	Color	Rh (%)	Color	Rh (%)
$Rh_4(CO)_{12}$/MCM-41	Brown	1.88	Pale	0.04
$Rh_4(CO)_{12}$/MCM-41(NH_2)				
First cycle	Brown	1.85	Brown	1.67
Second cycle	Brown	1.67	Brown	1.65
Third cycle	Brown	1.65	Brown	1.65
$Rh_4(CO)_{12}$/MCM-41(PPh_2)	Deep brown	1.86	Light yellow	0.07
$Rh_4(CO)_{12}$/MCM-41(SH)	Yellow	1.90	Yellow	1.90

When $Rh_4(CO)_{12}$/MCM-41 was used as a catalyst precursor, good catalytic performances were also achieved. However, it was noted that the solid sample completely decolorized (as pale as the MCM-41 support) and the color of liquid phase turned light red after reaction, indicative of the complete leaching of rhodium carbonyls from the MCM-41 support. Elemental analysis indicated that only 0.04% of Rh was retained on the solid sample after reaction. The easy loss of catalytic components in this case can be anticipated as the physisorbed rhodium carbonyls as they are readily extracted by THF. The rhodium carbonyls leaching into the liquid phase are most likely to be responsible for catalytic cyclohexene hydroformylation. The observed catalytic behavior is compatible with that of the $Rh_4(CO)_{12}$-derived homogeneous catalyst.

By contrast, a $Rh_4(CO)_{12}$/MCM-41(PPh_2)-derived catalyst presented a turnover of only 440 mol/mol Rh for cyclohexene conversion in the first reaction cycle. After the first cycle the solid sample color turned light yellow and the liquid phase color became brown. The light yellow solid sample contained only 0.07% of Rh, so that its conversion of cyclohexene declined to 0.8% in the second cycle. The results show that the surface phosphine has a negative effect on the activity and immobilization of rhodium carbonyls in cyclohexene hydroformylation. In the case of a $Rh_4(CO)_{12}$/MCM-41(SH)-derived catalyst, neither catalytic activities nor leaching of rhodium species were detected, as seen in Tables 3 and 4. This implies that the surface thiol deactivates rhodium carbonyls for cyclohexene hydroformylation via the strong coordinative bonding with the rhodium center.

It is intriguing to compare the catalytic behaviors of the catalyst systems studied as a function of reaction time during the formation of cyclohexane carboxaldehyde. As shown in Fig. 7, the curve of the $Rh_4(CO)_{12}$ system represents a typical homogeneous catalytic behavior: the catalyst was active to give a turnover of 1785 mol/mol Rh for aldehyde formed in the first 9 h, after which it became inactive. Evidently, the $Rh_4(CO)_{12}$/MCM-41 system behaved similarly to the $Rh_4(CO)_{12}$ system. This further demonstrates that the $Rh_4(CO)_{12}$-derived MCM-41-supported rhodium carbonyl species does not act as a heterogeneous catalyst, but is leached into the liquid phase instead during cyclohexene hydroformylation. In contrast, the $Rh_4(CO)_{12}$/MCM-41(NH_2) system

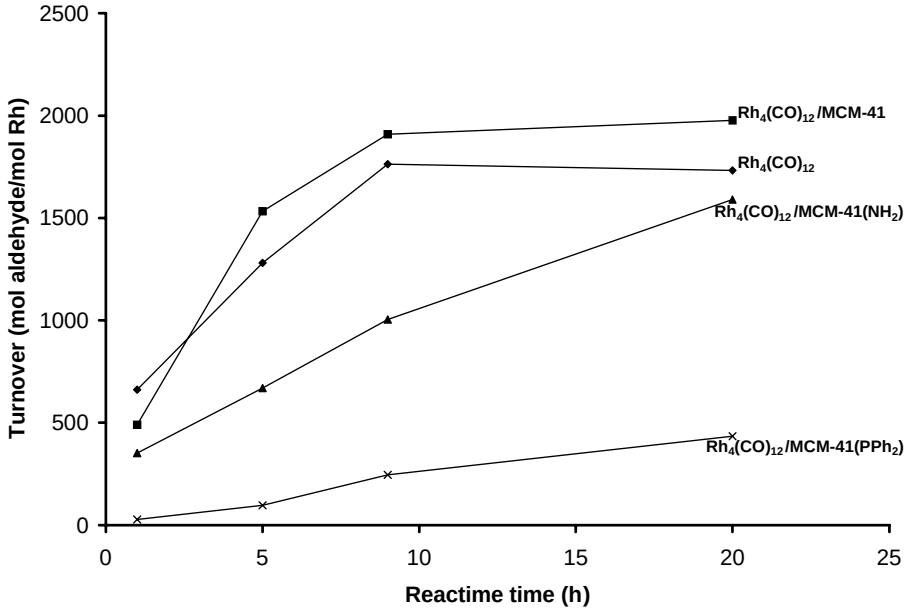

Fig. 7. Turnovers of cyclohexane carboxaldehyde formed as a function of reaction time over $Rh_4(CO)_{12}$-derived catalysts.

showed slightly lower catalytic activities to aldehyde than the $Rh_4(CO)_{12}$ system within 20 h of reaction, but the turnover of aldehyde formed increased continuously with increasing reaction time. The $Rh_4(CO)_{12}$/MCM-41(PPh_2) system exhibited much lower catalytic activities to aldehyde, the turnover of aldehyde formed still increasing with increasing reaction time. These facts illustrate that the rhodium catalytic species tethered on the functionalized MCM-41, though less active than the homogeneous rhodium catalyst within a short time, are stabilized by complexation of amine and phosphine ligands to different extent and remain active throughout the reaction and that the homogeneous catalytic species derived from $Rh_4(CO)_{12}$ completely deactivates after 9 h of reaction under 2.7 MPa of ($CO + H_2$) and at 100 °C. It is noteworthy that the turnovers of aldehyde formed increased well linearly with increasing reaction time after an induction period in the second and third cycles over $Rh_4(CO)_{12}$/MCM-41(NH_2), as shown in Fig. 8. At the end of the third cycle, the turnover exceeded that over $Rh_4(CO)_{12}$. This indicates that the $Rh_4(CO)_{12}$/MCM-41(NH_2)-derived catalyst can maintain good activity under steady reaction conditions. Thus, the MCM-41(NH_2)-tethered rhodium catalyst exhibits the advantages of better stability and potential longer lifetime for a prolonged pressurized reaction over the homogeneous rhodium catalyst.

Earlier investigations have attempted to develop rhodium carbonyl complexes linked to SiO_2 via phosphine, amine and thiol ligands, which are heterogeneous catalyst precursors for the liquid phase hydroformylation of hexene-1 [19,20]. The phosphine series employed $SiO_2(PPh_2Rh(acac)(CO))$, $((SiO_2(PPh_2))_3RhCl$, $((SiO_2(PPh_2))_2RhCl(CO)$ and $((SiO_2(PPh_2))_3RhH(CO)$ as catalyst precursors. Catalyst precursors for the amine and thiol series were $SiO_2(NH_2RhCl(CO)_2)$ and $([SiO_2\ (SRh(CO)_2)]_2 + SiO_2(SRh_2(CO)_4Cl)$. Based on the catalytic test results, it was believed that phosphine-bonded rhodium complex catalysts have the highest activity and better or accepted resistance to rhodium leaching, and that thiol-bonded rhodium complex catalysts possess no or the lowest activity depending on the reaction temperature and the highest retention of the rhodium [19,20]. Amine-bonded rhodium complex catalysts were thought to not only be less active than phosphine-bonded rhodium complex catalysts but have higher rhodium leaching [19,20]. But on the other hand, nitrogen-containing ligands like amines,

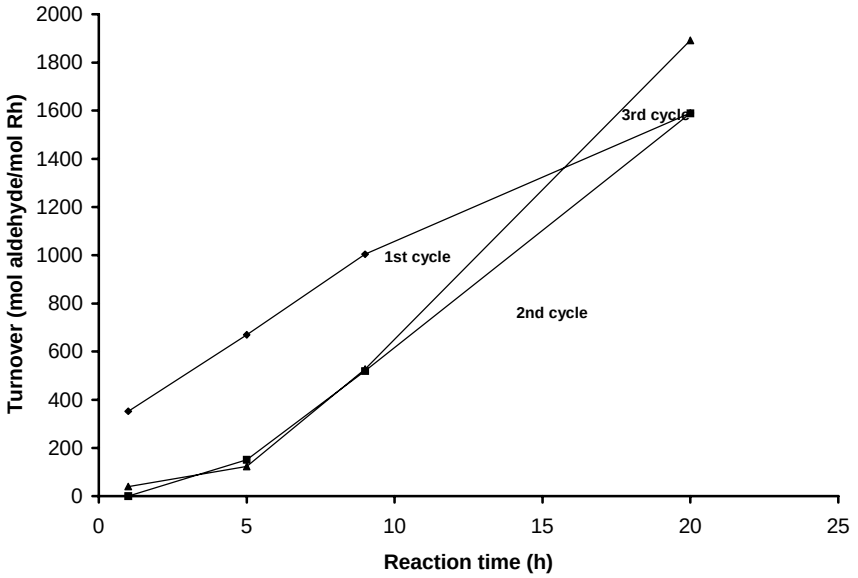

Fig. 8. Turnovers of cyclohexane carboxaldehyde formed as a function of reaction time over a $Rh_4(CO)_{12}$/MCM-41(NH_2)-derived catalyst.

amides and isonitriles show exclusively lower reaction rates in the oxo reaction due to their stronger coordination to the metal center [10]. In contrast to what was concluded previously with SiO_2-linked rhodium complex catalysts via phosphine and amine ligands for hydroformylation of hexene-1, our MCM-41-tethered rhodium carbonyl catalyst via an amine ligand shows marked advantages in both activity and stability over that via a phosphine ligand for hydroformylation of cyclohexene. In accordance with the previous results with SiO_2-linked phosphine-free rhodium complex catalysts via a thiol ligand [19,20,44], our MCM-41-tethered rhodium carbonyl catalyst via a thiol ligand exhibits no activity and the lowest rhodium loss in hydroformylation of cyclohexene.

Actually, the mesoporous features of silicate MCM-41 make no difference from amorphous SiO_2 in the basic chemical properties of silanol groups for linking organosilane coupling reagents via silylation. The catalytic properties and stability of such tethered catalysts are virtually dependent on the nature of chemical bonding of donor ligands with the metal center. Rhodium complexes thus supported on MCM-41 and on SiO_2 practically become gigantic donor ligand-containing rhodium complexes. Except for phosphine-coordinated metal complex catalysts, the relationship between the catalytic performances and the coordination of amine and thiol ligands toward hydroformylation is poorly established. Moreover, there is a lack of comparative information concerning the influences of these types of ligands on catalysis in the literature. From the point of view of fundamental coordinative bonding, $(O_s)_3Si(CH_2)_3PPh_2$ is a strong σ-electron donor and a poor π-electron acceptor, whereas $(O_s)_3Si(CH_2)_3SH$ is both strong σ-electron donor and a strong π-electron acceptor in donor ligand-containing metal complexes. Consequently, CO ligands are bonded more strongly to the metal center in the case of $(O_s)_3Si(CH_2)_3PPh_2$-containing metal complexes since the transition metal tends to transfer the increased negative charge from the phosphorus to CO or other ligands by π-back donation. This leads to increased stability of CO–M bond and thus decreased catalytic activity for hydroformylation compared to the phosphine-free metal complex. At the same time, the weaker dπ–pπ bonding between the metal center and the phosphorus results in decreased strength of P–M bond. In the case of $(O_s)_3Si(CH_2)_3SH$, contrarily, coordination of a thiol ligand to the metal center weakens the CO–M bond and in some cases causes the oxidation of metal center, in favor of the enhancement of S–M bond strength because of the stronger

dπ–pπ bonding between the metal center and the sulfur. This is reflected in the reactivity of supported thiol ligand with $Rh_4(CO)_{12}$, as studied by IR spectroscopy. The stronger S–Rh bond and formation of Rh^+ center in $[Rh(\mu\text{-}S(CH_2)_3Si(O_s)_3)(CO)_2]_2/SiO_2$ without strong electron-donating ligands like phosphines lead to no catalytic activity for hydroformylation. This state of sulfur-bonded rhodium center cannot change during a prolonged hydroformylation, even under pressurized $CO + H_2$ and at higher temperatures. As for amine-coordinated metal complexes, $(O_s)_3Si(CH_2)_3NH_2$ is only a strong σ-electron donor without dπ orbitals. However, the nitrogen is one of the most electronegative elements. In the presence of a coordinated amine, the metal center may transfer only a part of the increased negative charge from the nitrogen to CO or other ligands by π-back donation. This appropriate coordination of amine may not only produce a suitable strength of CO–M bond for hydroformylation but ensure the stability of N–M bond. The IR spectroscopic results suggest that the CO–Rh bond is weaker in the amine-coordinated rhodium carbonyls than in the phosphine-coordinated rhodium carbonyls. From the fact that the MCM-41(NH_2)-tethered rhodium carbonyl catalyst shows a weak and controllable rhodium leaching whereas the MCM-41(PPh_2)-tethered rhodium carbonyl catalyst exhibits a heavy rhodium leaching during cyclohexene hydroformylation, we speculate that the N–Rh bond is stronger than the P–Rh bond.

To explain the effect of donor ligands on the immobilization of rhodium complexes under hydroformylation conditions, we should take into account the associative and dissociative mechanisms of rhodium-catalyzed olefin hydroformylation proposed by Wilkinson and co-workers [8,57,58]. In the absence of excess donor ligands like PPh_3 and/or in the presence of high CO pressure, the hydroformylation reaction proceeds by the dissociative mechanism. A donor ligand is lost from the hydridic complex prior to olefin attack. On the other hand, the dissociation of such a ligand occurs and is displaced by CO by high reaction temperature, high CO pressure and low ligand/Rh ratios [58,59]. Under identical hydroformylation conditions, whether the rhodium center can re-coordinate the lost ligand or not relies on the complexation ability of the ligand with respect to CO. It follows that stabilization of MCM-41-tethered rhodium complex hydroformylation catalysts is correlated to characteristics of different donor ligands. Since the S–Rh bond in the MCM-41(SH)-tethered rhodium carbonyl catalyst is very strong, the catalyst is inactive for cyclohexene hydroformylation and the rhodium is well retained on the support during the reaction. As far as the MCM-41(NH_2)- and MCM-41(PPh_2)-tethered rhodium carbonyl catalysts are concerned, the former maintains fair catalytic stability without obvious rhodium loss during the reaction, which is attributed to the properly strong N–Rh bond; the latter has no catalytic stability with enormous rhodium loss during the reaction, which is related to the fragile P–Rh bond.

Finally, it is important to mention that the XRD spectrum of the $Rh_4(CO)_{12}$/MCM-41(NH_2)-derived catalyst maintained the initial peak intensities for mesoporous MCM-41 after the third reaction cycle. This demonstrates that the mesoporous structure of the MCM-41-based catalysts is not affected by operating catalytic conditions.

It is known that cyclic olefins hydroformylate more slowly than terminal olefins and that cyclic olefin hydroformylation is carried out at higher pressures or higher temperatures. According to Brown and Wilkinson, cyclohexene shows no hydroformylation at all under mild conditions [57]. At 12.7 MPa, with no ligand added, it reacts ten times as slowly as terminal olefins [60]. It is also documented that olefin hydroformylations over anchored rhodium complex catalysts are generally performed under high pressures of CO and H_2 (normally over 4.0 MPa) and at a temperature of 100 °C or above [5,36,37,61–63], except for a few particular examples with terminal olefins that can proceed under low pressures and at temperatures at below 100 °C [41,44,64]. By contrast, our $Rh_4(CO)_{12}$-derived MCM-41(NH_2)-tethered catalyst possesses quite remarkable catalytic properties for cyclohexene hydroformylation at merely 2.7 MPa of equimolar CO and H_2 and at 100 °C.

Table 5 compares the catalytic properties of our tethered catalyst and a number of rhodium-based heterogeneous catalysts reported to date for cyclohexene hydroformylation. Obviously, the $Rh_4(CO)_{12}$-derived MCM-41(NH_2)-tethered catalyst presents the highest activity under milder conditions among all the catalysts.

Table 5
Comparison of catalytic performances of various rhodium-based catalysts in cyclohexene hydroformylation

Catalyst precursor	Reaction time (h)	Activity[a] (mol/(mol Rh h))	Selectivity[a] (mol%)	Conditions	Reference
$Rh_4(CO)_{12}$/MCM-41(NH_2)	1	352	100	100 °C, 2.7 MPa, $H_2/CO = 1$	This work
	5	134	97	100 °C, 2.7 MPa, $H_2/CO = 1$	This work
	20	81	98	100 °C, 2.7 MPa, $H_2/CO = 1$	This work
$Rh_2Co_2(CO)_{12}$/Dowex MWA-1	3	28	85	100 °C, 6.7 MPa, $H_2/CO = 1$	[2]
	16	5	Unknown	100 °C, 4.9 MPa, $H_2/CO = 1$	[7]
($RhCl_3$-aliquat 336)/SiO_2	13.5	127	Unknown	134 °C, 4.0 MPa, $H_2/CO = 1$	[9]
$RhCl_3/SiO_2(Me_3N^+)$	4	4	Unknown	134 °C, 4.0 MPa, $H_2/CO = 1$	[9]
$Rh_2(CO)_2(P[C(Me)_3]_3)_2$ –(μ-Cl)(μ-$S(CH_2)_2Si(O_s)_3$)/SiO_2	15	6	Unknown	120 °C, 7.9 MPa, $H_2/CO = 1$	[4]
$Rh_2(CO)_2(P[C(Me)_3]_3)_2$ –(μ-Cl)(μ-$S(CH_2)_3Si(O_s)_3$)/SiO_2	15	5	Unknown	120 °C, 7.9 MPa, $H_2/CO = 1$	[4]
$Rh_2(CO)_2(P[C(Me)_3]_3)_2$ –(μ-Cl)(μ-$S(CH_2)$)/polymer	6	4	Unknown	120 °C, 7.9 MPa, $H_2/CO = 1$	[5]

[a] Cyclohexane carboxaldehyde + alcohols.

4. Conclusions

$Rh_4(CO)_{12}$-derived rhodium carbonyls have been successfully anchored to MCM-41(PPh_2), MCM-41(NH_2) and MCM-41(SH), which are formed, respectively, by functionalization of silicate MCM-41 with $Cl(CH_2)_3Si(OMe)_3$ plus $KPPh_2$, $H_2N(CH_2)_3Si(OEt)_3$ and $HS(CH_2)_3Si(OMe)_3$, to produce MCM-41-tethered unidentified phosphine- and amine-containing rhodium carbonyl clusters and MCM-41-tethered $[Rh(\mu\text{-}S(CH_2)_3Si(O_s)_3)(CO)_2]_2$. $Rh_4(CO)_{12}$ is mostly converted to $Rh_6(CO)_{16}$ on unfunctionalized MCM-41. The functionalization of MCM-41 and the subsequent grafting of rhodium complexes do not alter the structural ordering of MCM-41. The only modification is that functionalized MCM-41 and Rh/functionalized MCM-41 give reduced pore sizes, total pore volumes and BET surface areas.

All the $Rh_4(CO)_{12}$-derived catalysts studied exhibit very high selectivity (>98%) for the formation of cyclohexane carboxaldehyde in cyclohexene hydroformylation at 2.7 MPa of equimolar CO and H_2 and at 100 °C. Although the homogeneous catalyst derived from $Rh_4(CO)_{12}$ is very active, it entirely deactivates after 9 h of reaction. The $Rh_4(CO)_{12}$-derived MCM-41-supported catalyst shows a complete leaching of rhodium carbonyl species from the support during the reaction. The functionalized MCM-41-tethered $Rh_4(CO)_{12}$-derived catalysts behave in different manners depending on the donor ligand used. The MCM-41(NH_2)-tethered catalyst is the most active among the three donor ligand-functionalized MCM-41-tethered catalysts. Its catalytic activity is maintained stable under steady reaction conditions despite that it is slightly lower than that of the homogeneous catalyst within 20 h of reaction. This catalyst does not deactivates after three reaction cycles and becomes more active than the homogeneous catalyst in the third cycle. Only a weak rhodium loss from the support is detected after the first cycle and the rhodium content is retained unchanged in the following cycles. The MCM-41(PPh_2)-tethered catalyst is much less active than the MCM-41(NH_2)-tethered catalyst. The rhodium is seriously leached from the support during the first cycle. The MCM-41(SH)-tethered catalyst is inactive and has no rhodium leaching during the reaction. The distinct catalytic behaviors of these tethered catalysts are undoubtedly associated with the strength of coordination of different donor ligands to the rhodium center. The amine is bonded to the rhodium center to such a extent that the tethered rhodium complex catalyst can be guarantied active enough and the rhodium leaching can simultaneously be avoided. Therefore, the MCM-41(NH_2)-tethered rhodium catalyst is of marked and potential advantage in activity, stability and recovery over the other donor ligand-functionalized MCM-41-tethered rhodium catalysts in hydroformylation.

Furthermore, the operating reaction conditions used in this work do not lead to a change in the mesoporous structure of MCM-41.

References

[1] P. Pino, C. Botteghi, Org. Synth. 57 (1977) 11, and references therein.
[2] G.E. Hartwell, P.E. Garrou, US Patent no. 4,144,191 (1979).
[3] P.W.N.M. van Leeuwen, C.F. Roobeck, J. Organomet. Chem. 258 (1983) 343.
[4] M. Eisen, J. Blum, H. Schumann, S. Jurgis, J. Mol. Catal. 31 (1985) 317.
[5] M. Eisen, T. Bernstein, J. Blum, H. Schumann, J. Mol. Catal. 43 (1987) 199.
[6] S.K. Cao, M.Y. Huang, Y.Y. Jiang, Polym. Bull. 19 (1988) 353.
[7] L. Alvila, T.A. Pakkanen, T.T. Pakkanen, O. Krause, J. Mol. Catal. 71 (1992) 281.
[8] D. Evens, J.A. Osborn, G. Wilkinson, J. Chem. Soc. A (1968) 3133.
[9] J. Blum, A. Rosenfeld, N. Polak, O. Israelson, H. Schumann, D. Avnir, J. Mol. Catal. A 107 (1996) 217.
[10] M. Beller, B. Cornils, C.D. Frohning, C.W. Kohlpaintner, J. Mol. Catal. A 104 (1995) 17.
[11] M. Lenarda, L. Storaro, R. Ganzerla, J. Mol. Catal. A 111 (1996) 203, and references therein.
[12] J.C. Bayon, C. Claver, A.M. Masdeu-Bulto, Coord. Chem. Rev. 193 (1999) 73.
[13] P.W.N.M. van Leeuwen, C. Claver, Rhodium Catalyzed Hydroformylation, Kluwer Academic Publishers, Dordrecht, 2000.
[14] A. Sayari, Chem. Mater. 8 (1996) 1840.
[15] A. Corma, Chem. Rev. 97 (1997) 2373.
[16] M. Nowotny, T. Maschmeyer, B.F.G. Johnson, P. Lahuerta, J.M. Thomas, J.E. Davies, Angew. Chem. Int. Ed. 40 (2000) 955.
[17] K.G. Alum, R.D. Hancock, I.V. Howell, S. Mckenzie, R.C. Pitkethly, P.J. Robinson, J. Organomet. Chem. 87 (1975) 203.
[18] I.V. Howell, R.D. Hancock, R.C. Pitkethly, P.J. Robinson, in: B. Delmon, G. James (Eds.), Catalysis: Heterogeneous and Homogeneous, Elsevier, Amsterdam, 1975, p. 349.
[19] R.D. Hancock, I.V. Howell, R.C. Pitkethly, P.J. Robinson, in: B. Delmon, G. James (Eds.), Catalysis: Heterogeneous and Homogeneous, Elsevier, Amsterdam, 1975, p. 361.
[20] K.G. Allum, R.D. Hancock, I.V. Howell, S. Mckenzie, R.C. Pitkethly, P.J. Robinson, J. Catal. 43 (1976) 322.
[21] K.G. Allum, R.D. Hancock, I.V. Howell, T.E. Lester, S. Mckenzie, R.C. Pitkenthly, P.J. Robinson, J. Catal. 43 (1976) 331.
[22] K. Kochloefl, W. Liebelt, H. Knozinger, J. Chem. Soc., Chem. Commun. (1977) 510.
[23] S.C. Brown, J. Evans, J. Chem. Soc., Chem. Commun. (1978) 1063.
[24] H. Knozinger, E. Rumpf, Inorg. Chim. Acta 30 (1978) 51.
[25] H. Knozinger, E.W. Thornton, M. Wolf, J. Chem. Soc., Faraday Trans. 1 (1979) 1888.
[26] R. Pierantozzi, K.J. McQuade, B.C. Gates, M. Wolf, H. Knozinger, W. Ruhmann, J. Am. Chem. Soc. 101 (1979) 5436.
[27] J.L. Bilhou, V. Bilhou-Bougnol, W.F. Graydon, J.M. Basset, A.K. Smith, J. Mol. Catal. 8 (1980) 411.
[28] T. Castrillo, H. Knozinger, J. Leito, M. Wolf, Inorg. Chim. Acta 44 (1980) L239.
[29] T.J. Pinnavaia, J.G.-S. Lee, M. Abedini, in: D.E. Leyden, W.T. Collins (Eds.), Silylated Surfaces, Gordon and Breach, London, 1980, p. 333.
[30] J. Evans, B.P. Gracey, J. Chem. Soc., Dalton Trans. (1982) 1123.
[31] A. Luchetti, D.M. Hercules, J. Mol. Catal. 16 (1982) 95.
[32] H. Schumann, G. Gielusek, S. Jurgis, E. Hahn, J. Pickardt, J. Blum, Y. Sasson, A. Zoran, Chem. Ber. 117 (1984) 2825.
[33] B. Marciniec, Z. Foltynowicz, W. Urbaniak, J. Perkowski, Appl. Organomet. Chem. 1 (1987) 267.
[34] U. Kiiski, T.A. Pakkanen, O. Krause, J. Mol. Catal. 50 (1989) 143.
[35] M.T. Hoffmann, S.M.C. Neiva, M.R. Martins, D.W. Franco, in: H.A. Mottola, J.R. Steinmetz (Eds.), Chemically Modified Surfaces, Elsevier, Amsterdam, 1992, p. 257.
[36] L. Hong, E. Ruckenstein, J. Mol. Catal. 90 (1994) 303.
[37] D. Cauzzi, M. Lanfranchi, G. Marzolini, G. Predieri, A. Tiripicchio, M. Costa, R. Zanoni, J. Organomet. Chem. 488 (1995) 115.
[38] C.-J. Liu, S.-G. Li, W.-Q. Pang, C.-M. Che, Chem. Commun. (1997) 65.
[39] X. Feng, G.E. Fryxell, L.-Q. Wang, A.Y. Kim, J. Liu, K.M. Kemner, Science 276 (1997) 923.
[40] M.L. Kantam, T. Bandyopadhyay, A. Rahman, N.M. Reddy, B.M. Choudary, J. Mol. Catal. A 133 (1998) 293.
[41] H. Gao, R.J. Angelici, Organometallics 17 (1998) 3063.
[42] H. Gao, R.J. Angelici, New J. Chem. 23 (1999) 633.
[43] H. Gao, R.J. Angelici, J. Mol. Catal. A 149 (1999) 63.
[44] H. Gao, R.J. Angelici, J. Mol. Catal. A 145 (1999) 83.
[45] H. Gao, R.J. Angelici, Organometallics 18 (1999) 989.
[46] S.-G. Shyu, S.-W. Cheng, D.-L. Tzou, Chem. Commun. (1999) 2337.
[47] A.M. Liu, K. Hidajat, S. Kawi, D.Y. Zhao, Chem. Commun. (2000) 1145.
[48] A.M. Liu, K. Hidajat, S. Kawi, J. Mol. Catal. A 168 (2001) 303.
[49] C.M. Crudden, D. Allen, M.D. Mikoluk, J. Sun, Chem. Commun. (2001) 1154.
[50] P. Chini, Chem. Commun. (1967) 440.
[51] W. Beck, K. Lottes, Chem. Ber. 94 (1961) 2578.
[52] J.L. Bilhou, V. Bilhou-Bougnol, W.F. Graydon, J.M. Basset, A.K. Smith, G.M. Zanderighi, J. Oranomet. Chem. 153 (1978) 73.
[53] A. Theolier, A.K. Smith, M. Leconte, J.B. Basset, G.M. Zanderighi, R. Psaro, R. Ugo, J. Organomet. Chem. 191 (1980) 415.
[54] L. Huang, Y. Xu, W. Guo, A. Liu, D. Li, X. Guo, Catal. Lett. 32 (1995) 61.

[55] E.S. Bolton, R. Havlin, G.R. Knox, J. Organomet. Chem. 18 (1969) 153.
[56] J.S. Beck, J.C. Vartuli, W.J. Roth, M.E. Leonowicz, C.T. Kresge, K.D. Schmitt, C.T.-W. Chu, D.H. Olson, E.W. Sheppard, S.B. McCullen, J.B. Higgins, J.L. Schlenker, J. Am. Chem. Soc. 114 (1992) 10834.
[57] C.K. Brown, G. Wilkinson, J. Chem. Soc. A (1970) 2753.
[58] G. Yagupsky, C.K. Brown, G. Wilkinson, J. Chem. Soc. A (1970) 1392.
[59] R.L. Pruett, J.A. Smith, J. Org. Chem. 34 (1969) 327.
[60] B. Heil, L. Marko, Chem. Ber. 102 (1969) 2238.
[61] H. Arai, J. Catal. 51 (1978) 135.
[62] C.U. Pittman Jr., A. Hirao, J. Org. Chem. 43 (1978) 640.
[63] F.R. Hartley, S.G. Murray, P.N. Nicholson, J. Mol. Catal. 16 (1982) 363.
[64] Ph. Kalck, F.S. Spirau, New J. Chem. 13 (1989) 515.